Energy Harvesting across Temporal Temperature Gradients using Vaporization

Charles Xiao[1], Nicholas D. Naclerio[1], and Elliot W. Hawkes[1]

***Abstract*— Energy harvesting is an attractive alternative to carrying onboard power for mobile robots, especially for long duration missions. While solar is a powerful option, alternatives are needed for situations where direct sunlight is unavailable. One intriguing concept was proposed in the 17th century to power clocks: energy harvesting based on temporal, rather than spatial, temperature gradients, using a low boiling point fluid that vaporizes at ambient temperatures. This concept has many strengths: it offers all-in-one energy harvesting and storage; it has direct high-power mechanical output, eliminating the need for a motor; and temporal gradients are ubiquitous, due to diurnal thermal fluctuations. The challenge for robotic applications, however, is to create large enough amounts of work in a small enough package to power a mobile device while using a non-toxic and readily available fluid. Here we present a simple, low-cost energy harvesting actuator, powered by the vaporization of butane and iso-butane, with an isobaric energy density of up to 38000 J/m^3 (i.e. energy extracted per total volume expansion) each time the temperature fluctuates 13.1° C, enough to power a small car to drive 10 m. Two principles enable this: i) precompression of the working fluid, allowing us to tune the boiling point and choose among many non-toxic fluids that do more work than non-compressed fluids; and ii) a constant force profile of the return springs, allowing more work than a linear spring. We present a simple model of the actuator and experimental results characterizing its behavior. Our work lays the foundation for energy harvesting across temporal temperature gradients using vaporization as a viable option for powering mobile robots.**

I. INTRODUCTION

Long term robotic missions including exploration and sensing require renewable energy sources, because it is impractical to carry the required fuel or batteries. Renewable sources such as wind [1] and solar [2] can be used, but they are limited to environments with direct sunlight or air flow. A promising alternative energy source for shaded environments such as urban centers, forests, and Martian dust storms, is thermal energy. Temporal temperature gradients are as ubiquitous as night and day, and are available in many environments.

Several previous studies have been able to harvest energy from daily temperature fluctuations using a variety of mechanisms. Some of the earliest examples are "perpetual motion" clocks such as Cornelius Drebbel's 17th centrury "perpetuum mobile," which led to Jean-Leon Reutter's 19th century "Atmos clock" [3]. The Atmos clock uses the expansion and contraction of vaporizing ethyl chloride in a sealed mechanical bellow over small variations in ambient temperature to wind a clock. Other modern methods have explored thermal resonance [4], pyroelectricity [5], solid to liquid phase transitions [6] and more [7], [8]. However, few modern studies have used liquid to gas phase transitions for energy harvesting like the Atmos clock due to the high pressures and volume changes involved [8].

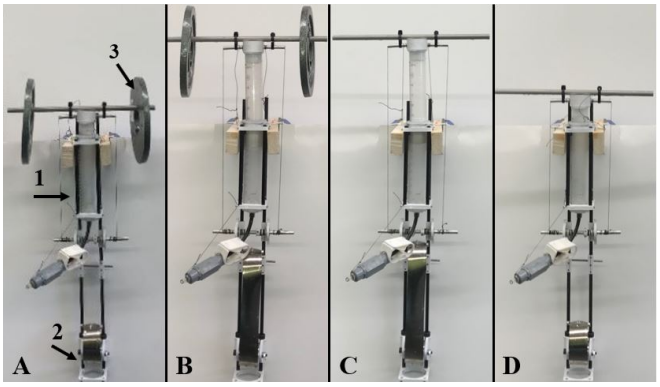

Fig. 1. Expansion and compression cycle of the actuator and spring system. **1** is the rolling diaphragm actuator, **2** is a constant force spring, and **3** is a mass weighing 22 N. (A) The loaded system at 5.5°C. (B) The loaded system at 20°C; a stroke of 10 cm was achieved. (C) The unloaded system still at 20°C. (D) The unloaded system again at 5.5°C, now compressed under the force exerted by the spring. Overall, 2.2 J of work was done by the cycle.

Vaporization is promising for providing both an energy source and direct mechanical power to small robots because of its high pressure and volume change. Liquid-vapor phase transitions have been utilized in several studies to create mechanical actuation, however they are generally very inefficient [9]. If however, the actuator itself harvests energy from the environment, this is less of an issue. A study by Ali et al [10] explored this idea for energy harvesting, using a similar mechanism as the Atmos clock to load a spring, but it was immobile and used hard to source materials such as ethyl chloride. The advantage of using vaporization as an energy harvesting method is that it combines the role of energy harvester, storage device (i.e. a type of steam accumulator), and mechanical actuator into one mechanism. Energy is absorbed as the fluid boils, stored in the latent heat of the vapor and liquid mixture, and spent as mechanical work when needed. For comparison, a conventional pneumatic device would require a power source, compressor, valves, and pneumatic actuator to do the same tasks. The challenge, however, is to realize this concept in an actuator that can

*The authors acknowledge support from the California NanoSystems Institute (CNSI) Challange Grant program.

[1]C. Xiao, N. Naclerio, and E. Hawkes are with the Department of Mechanical Engineering at the University of California Santa Barbara, Santa Barbara, USA. (Emails: charles_xiao@ucsb.edu; nnaclerio@ucsb.edu; ewhawkes@ucsb.edu)

power a mobile robot while in a form factor that can be carried on board.

To address this challenge, the primary contribution of this work is an actuator capable of powering a mobile robot (here, a simple car) by harvesting energy from temporal temperature gradients by using readily available, inexpensive, non-toxic working fluids. We realize this with two principles: precompressing the working fluid, and using a constant force return spring. Precompression allows the boiling point of the working fluid to be tuned to a given environment, maximizing the energy absorbed for a small temperature fluctuation, while allowing us to choose any working fluid that has a boiling point below our target temperature range. The constant force return spring allows us to theoretically harness up to twice the energy of a system using linear springs. This allows us to extract up to 0.038 J/ml of vaporized butane fuel over a 13.1 °C temperature change for an isobaric cycle. What follows is a a brief analytical model and description of our design, an experimental characterization of its properties, and a demonstration of its potential for use in energy harvesting robots by powering a prototype wheeled vehicle 10 m over a 16 °C temperature change.

II. Working Theory

This section describes the thermodynamics governing the behavior of our device.

A. Cycle Work

The amount of work done by a gas is given by the expression:

$$W = \int_V P_g dV \tag{1}$$

where P_g is the absolute pressure of the gas and dV is the change in volume. Expansion occurs when the pressure of the gas exceeds the applied pressure P_{ex}, and compression occurs if the applied pressure exceeds the pressure of the gas. The applied pressure can be decomposed into the atmospheric pressure P_{atm}, the restoring element (e.g., preload spring) P_s, and the load P_l. P_{atm} and P_s can be combined to form an effective atmosphere term P_{ea}, such that

$$P_{ex} = P_{atm} + P_s + P_l = P_{ea} + P_l. \tag{2}$$

Expansion work is maximized if it is done at constant pressure at the highest pressure achievable by the gas. For the vaporization of a volatile liquid at constant pressure, the following expression gives the maximum possible work done.

$$W = P(V_f - V_i) \approx P\frac{nRT}{P} = nRT, \tag{3}$$

where V_f and V_i are the final and initial volumes respectively, n is the moles of liquid evaporated, R is the ideal gas constant, and T is the absolute temperature at the end of the expansion. The terms to the right of the approximation were written by assuming that the evaporated gas behaves ideally and that the initial liquid volume is small in comparison to the final gaseous volume.

Not all the work, however, goes toward moving the load; a large portion of it goes towards moving the atmosphere and restoring elements, which allows the system to cycle back to its initial volume once sufficient cooling has occurred. For mechanical simplicity, the cycle chosen for analysis is a constant pressure cycle. Energy is harvested during the expansion. Using the small initial volume assumption, the net work (i.e., the work that goes into the load) evolved during the cycling is

$$W = nRT\frac{P_l}{P_{ea} + P_l}. \tag{4}$$

B. Maximizing Work Output

Increasing T and/or n increases the work done in the cycle. A higher T results in a greater pressure difference between the hot and cold states because of two related effects: increased evaporation (i.e. greater n) and more energetic gas molecules. As a result, more work can be done. In many temporal systems, however, it is not possible to increase the maximum temperature of the system; thus, n must be improved. In general, selecting a fluid of a lower boiling point allows for greater evaporation at a given temperature, because the vapor pressure of a fluid increases nearly exponentially after the boiling point (see Fig. 2).

Table I provides some working fluid properties and calculations for an ideal system that operates between 10 and 20°C. Italicized fluids are ones that could be found at a local hardware store (note that butane is often mixed with iso-butane). The column on the far right gives the energy density of the working fluids, which is equivalent to the pressure difference between the hot and cold states. From the table it can be seen that an energy harvesting system, that uses butane will ideally do about 1.5 times more work than a system that uses ethyl chloride for a given volume change, and a system that uses iso-butane will ideally do more than 2.2 times more work.

C. Non-Idealities

Two sources of non-idealities are discussed in this section: residual air and mixed working fluids. Residual air is the gas inside the system that does not come from the working fluid. As long as the overall pressure is low and the residual air is non-interacting, it can be reasonably assumed that it behaves ideally; thus, its presence leads to pressure drops during expansion and pressure increases during compression.

Mixed working fluids are working fluids that contain two or more chemicals. Such fluids are encountered if the fluids are non-laboratory grade, such as butane fuel (usually a mixture of iso-butane and butane). If the two components are sufficiently non-interacting, as in the case of iso-butane and butane, then it can be assumed that the fluid behaves ideally [11]. The vapor pressure of an ideal mixture is described by combining Raoult's law with Dalton's law of partial pressure, which yield a relationship stating that the pressure exerted by the fluid's vapor, P_f is

$$P_f = \sum \chi_i P_i, \tag{5}$$

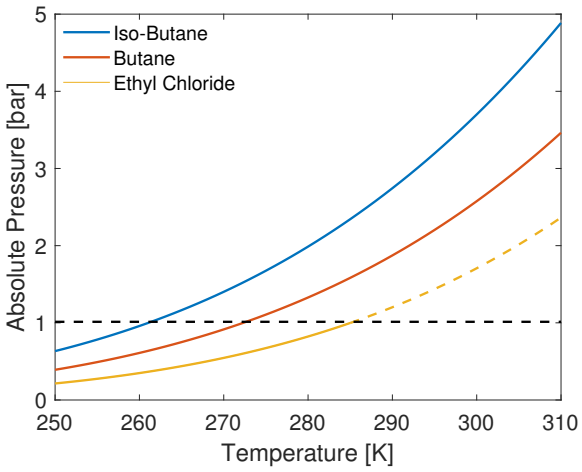

Fig. 2. Plot of the vapor pressure of butane [13], iso-butane [13], and ethyl chloride [16]. The dashed portion of the ethyl chloride line is outside the range of the Antoine Equation. The dashed black line is atmospheric pressure at sea level.

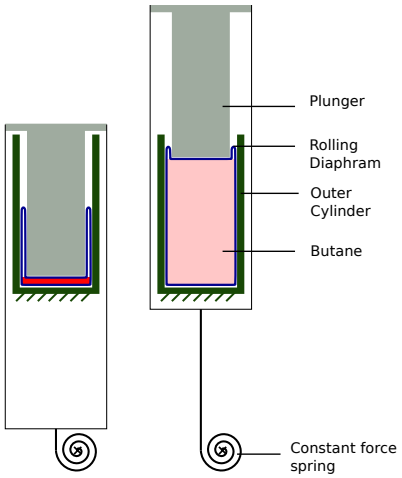

Fig. 3. The energy harvesting actuator shown in its compressed state on the left, and expanded state on the right. As the butane (in red) vaporizes, it drives the piston up, extending the constant force spring.

where χ_i is the mole fraction of the i component of the fluid and P_i is its vapor pressure [12]. It is important to note that the composition of the fluid changes during expansion and compression. In a closed non-reacting system the total moles, $n_{i,total}$, of a chemical remains constant. This can be described by

$$n_{i,total} = \frac{n_i}{\sum n_i} P_i \frac{V}{RT} + n_i, \tag{6}$$

where n_i is the molar amount of i in the liquid and $\frac{n_i}{\sum n_i} P_i \frac{V}{RT}$ is the amount of i in the gas. If only a small amount of liquid is vaporized or condensed, as is the case for the systems described in Sec. IV, then the change in fluid composition and vapor pressure is small during the cycle.

III. Design

A. Energy Harvesting Actuator

The energy harvesting actuator consists of a pneumatic piston filled with butane fuel, and a constant force return spring. As the butane heats and expands, it drives the actuator. As it cools, the spring returns it to a compressed state.

The prototype pneumatic actuator consists of a thin, flexible, rolling diaphragm, a rigid outer cylinder, and a rigid piston as in Fig. 3. The rolling diaphragm is made from thin lay-flat polyethylene tubing; the casing and piston is made with polypropylene. All three components were chosen for their low cost and compatibility with butane fuel. The butane (Bernzomatic) comes from a canister for refueling lighters. As the butane expands, it pressurizes the bladder, forcing the piston out of the cylinder. This rolling diaphragm method was chosen over a traditional pneumatic piston or metal bellow, because of its low cost, low stiction, and low to no leak rate. The 65.7 N constant force spring is mounted below the actuator, and connected to the piston by spectra fishing line such that it extends as the actuator expands (see Fig. 3). The diameter of the piston is 30.3 mm with room for 10 cm of travel. The overall height and width of the compressed actuator (without spring) are 20 cm and 4 cm respectively, and its weight is 225 grams.

B. Prototype Energy Harvesting Wheeled Vehicle

To demonstrate a potential application of the phase change actuator, it was implemented in a simple wheeled vehicle. The car features a frame of carbon fiber rods with 3D printed polylactic acid (PLA) braces on which the energy harvester as described in Sec. III-A, a gear reduction, and wheels are mounted (see Figures 4 and 8). The actuator piston is attached at one end of the frame, with the return spring at the other, connected by spectra fishing line to a pulley between them, such that as the piston expands, it pulls on the 65.7 N constant force spring. A 160 tooth timing belt pulley with a one way bearing is also attached to the pulley, such that it rotates as the piston expands, but does not as it contracts. The pulley is connected to a 10 tooth pulley on the drive axle, connected to 12 cm diameter drive wheels. As such, the car ideally drives 302 cm for every cm that the piston expands. The car's length is 50 cm, and its height is 14 cm.

IV. Results

A. Actuator Characterization: Pressure-Volume Data

The relationship between pressure, temperature, and time was experimentally characterized to evaluate the effectiveness of the actuator's thermal cycle.

The piston was tested on a mechanical test stand with manually controlled displacement. The high temperature of the piston was controlled by exposing the piston to ambient air (26.9 °C), and its low temperature was achieved by submerging the piston in a manually controlled ice water bath of 13.8 °C. The piston was loaded with commercially available butane fuel, which contains both iso-butane and n-butane. To simulate quasi-static displacement, the actuator was allowed to expand to a known displacement and then

TABLE I

WORKING FLUID PROPERTIES AND CALCULATIONS

Fluid	B.P. [$^\circ C$]	$P(10^\circ C)$ [bar]	$P(20^\circ C)$ [bar]	J/m^3
Propane[13]	-42.11	6.37	8.37	200000
Ammonia [13]	-33.33	6.15	8.57	240000
R134A[14][15]	-26.3	4.15	5.72	160000
Iso-Butane [13]	-11.75	2.21	3.02	82000
Butane [13]	-0.49	1.49	2.08	59000
Neopentane [13]	9.5	1.03	1.46	43000
Ethyl Chloride [16]	12.3	0.93	1.35	42000

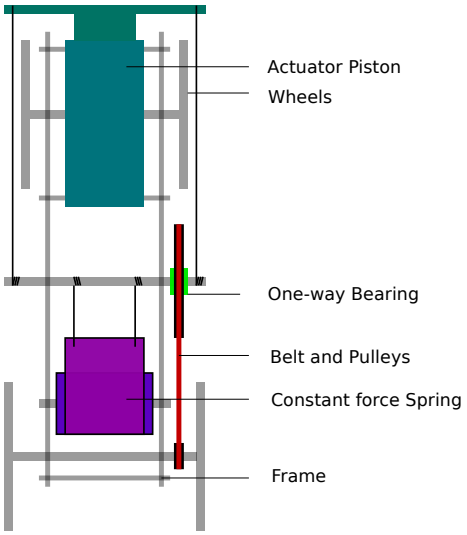

Fig. 4. Schematic of the wheeled vehicle powered by the energy harvesting actuator.

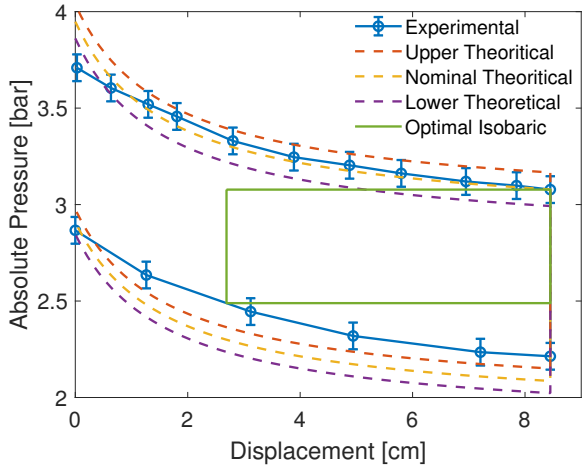

Fig. 5. The actuator's Pressure-Volume Diagram. The error bars come from the the uncertainty (∼6.9 kPa) in the pressure sensor used. The experimental data was compared to fitted theoretical models.

the motion was stopped to allow the pressure to settle. The resulting pressure and force data are plotted in Figures 5 and 6, respectively. The total amount of possible work enclosed in Figures 5 and 6 are 5.0 and 4.9 J, respectively.

The experimental data in Fig. 5 was compared to a fitted model. An estimate for the composition of the fluid was obtained by solving for the mole fraction of iso-butane at the point of maximum expansion ($\chi_{iso} = 0.32$). The upper and lower models account for the thermometer's uncertainty (1.0 K). Most importantly, the model accounts for the approximately 11 ml of residual air between the pressure sensor and the actuator. This explains the curvature seen in the experimental data; without the residual air, the system would be close to isobaric. Additionally, it reduces the maximum constant load that the actuator can move through a given stroke. For example, the optimal isobaric cycle that can be constructed for this system could only do 2.3 J over a stroke of 5.8 cm. Therefore, for constant load applications, it is essential to remove residual air if possible work is to be maximized. Note, however, that the total possible work done by a system with residual air and one without is similar as long as the absolute temperature of the cold and hot states are close. For example, the work done by the nominal theoretical model with residual air is 5.7 and without it and under isobaric conditions is also 5.7.

Fig. 6 compares the experimentally measured force with the force predicted by the pressure measurements. As expected, the total possible work done by the actuator (4.9 J) is lower than the work predicted by the pressure measurements (5.0 J). The similarity in values suggests low hysteresis and friction in the actuator. Greater losses are expected in the actuator in non-quasi static cases as viscous effects become important.

B. Power Analysis

The amount of power that an actuator can deliver is an important parameter for many applications.

To measure the power of the actuator, the actuator was allowed to freely expand and lift a weight of 120 N in a setup similar to the one shown in Fig. 1. Instead of a spring, a weight of 92 N was used as the restoring element; thus, the actuator does work on a load of $120\,\text{N} - 92\,\text{N} = 28\,\text{N}$. Power was calculated by multiplying the load with velocity. The position of the load was determined with a camera and the velocity was determined by taking the numerical time derivative of position. Fig. 7 shows how the pressure, power, and displacement varies with time. A maximum velocity of 5.6 mm/s was measured, resulting in a maximum power of approximately 160 mW. Maximum power is delivered early

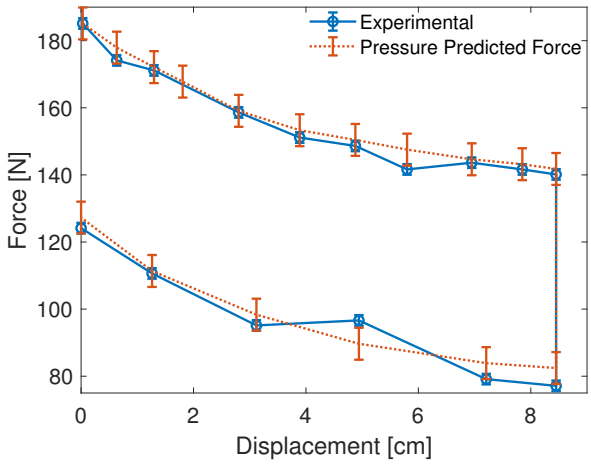

Fig. 6. The actuator's Force-Displacement Diagram. The error bars come from the force sensor's uncertainty (1.6 N), and they are similar in size to the markers. The error bars in the pressure predicted force curve comes from the uncertainty in the pressure measurement. The predicted and experimental curves were matched in magnitude at the first point of the expansion phase.

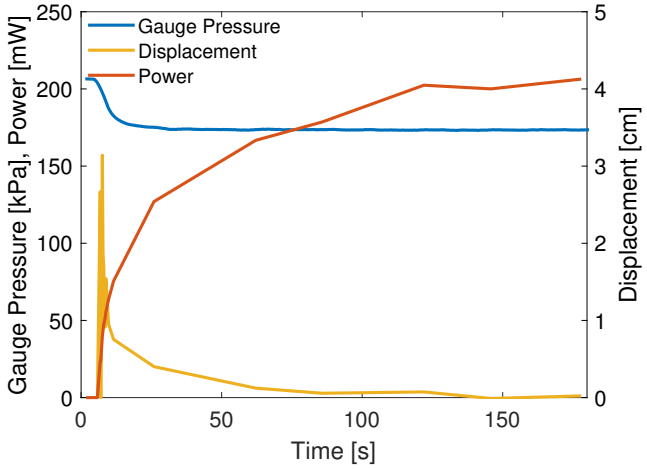

Fig. 7. Pressure, power, and displacement during the power test.

during the expansion phase, because residual air results in greater pressures at the beginning of the stroke.

C. Actuator Characterization: Full System Test

The entire energy harvesting actuator with a constant force return spring was tested with a mass lifting experiment. The setup is the same as the one shown in Fig. 1. The warm and cold bath temperatures were 20.0 °C and 5.5 °C, respectively, and the load added during expansion was 22 N, while the added load under compression was zero.

The work done by the phase change actuator on the weight was 2.2 J, giving an energy density of 0.030 J/ml.

D. Example Application: Wheeled Vehicle

The wheeled vehicle, as described in Sec. III-B and shown in Fig. 8 was able to travel about 10 m by harvesting thermal energy from a 16 °C temperature change by moving from a 4 °C environment to a 20 °C smooth floored hallway.

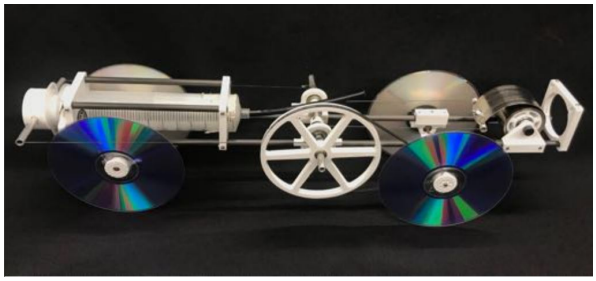

Fig. 8. Photo of the wheeled vehicle powered by the energy harvesting actuator. Its height and length are 14 cm and 50 cm, respectively.

V. Discussion

A. Working Fluids

While fluids such as neopentane and ethyl chloride have convenient boiling points at around 10°C, they are not ideal chemicals for harvesting diurnal energy harvesting. These chemicals are slightly toxic and not readily available. Here we show that the boiling point of the working fluid can be tuned through compression. This opens up the design space to many commonly available fluids. Additionally, low boiling points have greater energy densities (see Table I and Sec. V-B). As an added benefit, fluids such as butane, R134A, and propane all have lower toxicity than ethyl chloride and neopentane [17] (although none of these chemicals is completely hazard free).

B. Energy Density Values

One way to characterize performance of an energy harvester or storage device is its energy density and specific energy. The actuator tested in Sec. IV-A produced maximum possible work of 4.9 J over a total expansion of 62 ml, giving a maximum energy density of 0.079 J/ml, and for the optimal isobaric case, an energy density of 0.038 J/ml. Note that energy density for a system without residual air should be close to 0.079 J/ml (see Sec. IV-A). Greater energy densities are achievable with other working fluids.

For example, propane in an energy harvesting system operating between 10 and 20°C, has an approximate energy density of about 0.20 J/ml and a specific energy of about 13 J/g. In comparison, a lead acid battery has an energy density between 126 and 144 J/g and a specific energy between 288 and 324 J/ml [18]. Unlike the lead acid battery, a gas phase change system can regenerate its energy and does not require additional actuators. Liquid to gas phase transitions may be attractive in cases where there are no volume constraints.

C. Potential Robotic Applications

The demonstrated car traveled about 10 meters. It is reasonable to believe that an optimized design would have traveled a much further distance, or a similar distance over more challenging terrain. An interesting case study is a small martian rover. Before Opportunity's demise due to a possible low power event caused by a dust storm, it had traveled 45.16 km over 5111 martian days, an average of 8.8 m a day [19]. Temperature measurements between sols 45 and

65 show an average diurnal variation between 185 K and 260 K [20]. An ideal 1 L sublimation of carbon dioxide at that temperature range would produce about 2400 J of usable work according to the ideal gas model in Sec. 4 and require about 48 g of dry ice. This energy could be used to quickly charge batteries after a dust storm to power communication equipment.

D. Energy Harvesting Applications

Another interesting comparison, is with solar panels. In general solar panels perform very well in direct sunlight, even in northern latitudes. For example, the area around New York City can expect an average solar energy production of 4.3-4.5 kWh/m^2/day [21], which is roughly a factor of 77 more energy than the ideal 1m^3 expansion that propane could produce. However, the performance of solar panels decline significantly in shaded conditions, especially in partial shade [22]. Urban environments have significant shading. A recent analysis of New York City, found that most Manhattan neighborhoods were covered in shadows for more than half the day [23]; thus, it is reasonable to estimate that the solar production resources in many areas of a city are cut by half. Furthermore, gas expanding devices can take advantage of the vertical axis. After accounting for these factors, then a gas expanding system might be competitive. For example, assuming sufficient daily heat transfer, a system expanding 10 cubic meters of propane on a 1 square meter footprint operating between 10 and 20 °C could produce about 0.56 kWh of energy in a shaded area. For comparison, a solar panel operating in an area with half the normal sunlight would produce around 2.22 kWh of energy. Phase change systems can be placed in underutilized spaces where solar power performs poorly such as alley ways, allowing for those spaces to take advantage of the sun's energy.

VI. Conclusion

This work introduces an energy harvesting actuator for mobile robots that uses vaporization of a working fluid to pull energy from temporal temperature gradients. Critically, we demonstrate that pre-compressing the working fluid enables cheap, common, low boiling point fluids to be easily used in this application. A prototype actuator powered by butane was constructed and able to produce a maximum work of 4.9 J and energy density of up to 0.085 J/ml, and it has a maximum isobaric work of 2.3 J and energy density of 0.38 J/ml The utility of such a system was demonstrated with a wheeled vehicle that traveled about 10 m. Future work will investigate other common low boiling point liquids, theorized to give even higher energy densities, and will seek to improve the efficiency of the actuator while better understanding the complex heat transfer of such systems.

ACKNOWLEDGMENTS

The authors would like to thank the Read Group for the use of their lab space to conduct experiments, and Jenny Walker for her work on the project that originated this paper.

References

[1] N. A. Cruz and J. C. Alves, "Autonomous sailboats: An emerging technology for ocean sampling and surveillance," in *OCEANS 2008*. IEEE, 2008, pp. 1–6.

[2] L. E. Ray, J. H. Lever, A. D. Streeter, and A. D. Price, "Design and power management of a solar-powered cool robot for polar instrument networks," *Journal of Field Robotics*, vol. 24, no. 7, pp. 581–599, 2007.

[3] S. Patel, D. Moline, and J. Wagner, "Modeling and analysis of an atmospheric driven atmos clock with mechanical escapement control," in *2013 European Control Conference (ECC)*. IEEE, 2013, pp. 281–287.

[4] A. L. Cottrill, A. T. Liu, Y. Kunai, V. B. Koman, A. Kaplan, S. G. Mahajan, P. Liu, A. R. Toland, and M. S. Strano, "Ultra-high thermal effusivity materials for resonant ambient thermal energy harvesting," *Nature communications*, vol. 9, no. 1, p. 664, 2018.

[5] A. Cuadras, M. Gasulla, and V. Ferrari, "Thermal energy harvesting through pyroelectricity," *Sensors and Actuators A: Physical*, vol. 158, no. 1, pp. 132–139, 2010.

[6] G. Wang, D. S. Ha, and K. G. Wang, "Harvesting environmental thermal energy using solid/liquid phase change materials," *Journal of Intelligent Material Systems and Structures*, vol. 29, no. 8, pp. 1632–1648, 2018.

[7] M. F. Demirbas, "Thermal energy storage and phase change materials: an overview," *Energy Sources, Part B: Economics, Planning, and Policy*, vol. 1, no. 1, pp. 85–95, 2006.

[8] H. Nazir, M. Batool, F. J. B. Osorio, M. Isaza-Ruiz, X. Xu, K. Vignarooban, P. Phelan, A. M. Kannan *et al.*, "Recent developments in phase change materials for energy storage applications: A review," *International Journal of Heat and Mass Transfer*, vol. 129, pp. 491–523, 2019.

[9] A. Miriyev, K. Stack, and H. Lipson, "Soft material for soft actuators," *Nature communications*, vol. 8, no. 1, p. 596, 2017.

[10] G. Ali, J. Wagner, D. Moline, and T. Schweisinger, "Energy harvesting from atmospheric variations–theory and test," *Renewable energy*, vol. 74, pp. 528–535, 2015.

[11] J. F. Connolly, "Ideality of n-butane:isobutane solutions," *The Journal of Physical Chemistry*, vol. 66, no. 6, pp. 1082–1086, 1962. [Online]. Available: https://doi.org/10.1021/j100812a028

[12] F. P. Incropera, A. S. Lavine, T. L. Bergman, and D. P. DeWitt, *Fundamentals of heat and mass transfer*. Wiley, 2007.

[13] Air LiquideAir Liquide, "Gas encyclopedia," 2019, vapor data retrieved from this database, https://encyclopedia.airliquide.com/.

[14] P. Inc., *Research Chemicals Catalog 1990-1991*. NIST.

[15] M.-S. Zhu, J. Wu, and Y.-D. Fu, "New experimental vapor pressure data and a new vapor pressure equation for hfc134a," *Fluid phase equilibria*, vol. 80, pp. 99–105, 1992.

[16] J. Gordon and W. Giauque, *The entropy of ethyl chloride. Heat capacity from 18 to 287K. Vapor pressure. Heats of fusion and vaporization*. NIST.

[17] Airgas, "Sds search," 2019.

[18] G. J. May, A. Davidson, and B. Monahov, "Lead batteries for utility energy storage: A review," *Journal of Energy Storage*, vol. 15, pp. 145–157, 2018.

[19] NASA. (2019) Opportunity updates. [Online]. Available: https://mars.jpl.nasa.gov/mer/mission/rover-status/opportunity/recent/all/?y=2019sols-5347

[20] M. D. Smith, M. J. Wolff, M. T. Lemmon, N. Spanovich, D. Banfield, C. J. Budney, R. T. Clancy, A. Ghosh, G. A. Landis, P. Smith *et al.*, "First atmospheric science results from the mars exploration rovers mini-tes," *Science*, vol. 306, no. 5702, pp. 1750–1753, 2004.

[21] Solar map. NREL. [Online]. Available: https://www.nrel.gov/gis/solar.html

[22] M. R. Maghami, H. Hizam, C. Gomes, M. A. Radzi, M. I. Rezadad, and S. Hajighorbani, "Power loss due to soiling on solar panel: A review," *Renewable and Sustainable Energy Reviews*, vol. 59, pp. 1307–1316, 2016.

[23] Q. Bui and J. White, "Mapping the shadows of new york city: Every building, every block," 2016.